This is a self-archived version of an original article. This version may differ from the original in pagination and typographic details.

Author(s): Juvonen, Risto O.; Heikkinen, Aki T.; Kärkkäinen, Olli; Jehangir, Rabia; Huuskonen, Juhani; Troberg, Johanna; Raunio, Hannu; Pentikäinen, Olli T.; Finel, Moshe

Title: In vitro glucuronidation of 7-hydroxycoumarin derivatives in intestine and liver microsomes of Beagle dogs

Year: 2020

Version: Accepted version (Final draft)

Copyright: © 2019 Elsevier B.V.

Rights: CC BY-NC-ND 4.0

Rights url: https://creativecommons.org/licenses/by-nc-nd/4.0/

Please cite the original version:

Juvonen, R. O., Heikkinen, A. T., Kärkkäinen, O., Jehangir, R., Huuskonen, J., Troberg, J., Raunio, H., Pentikäinen, O. T., & Finel, M. (2020). In vitro glucuronidation of 7-hydroxycoumarin derivatives in intestine and liver microsomes of Beagle dogs. European Journal of Pharmaceutical Sciences, 141, Article 105118. https://doi.org/10.1016/j.ejps.2019.105118

Journal Pre-proof

In vitro glucuronidation of 7-hydroxycoumarin derivatives in intestine and liver microsomes of Beagle dogs

Risto O. Juvonen , Aki T. Heikkinen , Olli Kärkkäinen ,
Rabia Jehangir , Juhani Huuskonen , Johanna Troberg ,
Hannu Raunio , Olli T. Pentikäinen , Moshe Finel

Please cite this article as: Risto O. Juvonen , Aki T. Heikkinen , Olli Kärkkäinen , Rabia Jehangir , Juhani Huuskonen , Johanna Troberg , Hannu Raunio , Olli T. Pentikäinen , Moshe Finel , In vitro glucuronidation of 7-hydroxycoumarin derivatives in intestine and liver microsomes of Beagle dogs, *European Journal of Pharmaceutical Sciences* (2019), doi: https://doi.org/10.1016/j.ejps.2019.105118

In vitro glucuronidation of 7-hydroxycoumarin derivatives in intestine and liver microsomes of Beagle dogs

[1]Risto O. Juvonen, [2]Aki T. Heikkinen, [1]Olli Kärkkäinen, [1]Rabia Jehangir, [3]Juhani Huuskonen, [4]Johanna Troberg, [1]Hannu Raunio, [5]Olli T. Pentikäinen, [4]Moshe Finel.

[1] School of Pharmacy, Faculty of Health Sciences, University of Eastern Finland, Box 1627, FI-70211 Kuopio, Finland

[2]Admescope Ltd, Oulu, Finland

[3] University of Jyvaskyla, Department of Chemistry, P.O. Box 35, FI-40014 University of Jyvaskyla, Finland

[4] Division of Pharmaceutical Chemistry and Technology, Faculty of Pharmacy, University of Helsinki, P.O. Box 56, FI-00014 University of Helsinki, Finland

[5] Institute of Biomedicine, Faculty of Medicine, University of Turku, FI-20014 University of Turku, Finland

Corresponding author: Risto O. Juvonen, risto.juvonen@uef.fi, School of Pharmacy, Faculty of Health Sciences, University of Eastern Finland, Box 1627, FI-70211 Kuopio, Finland

Declaration of interest: none

Abstract

Beagle dog is a standard animal model for evaluating nonclinical pharmacokinetics of new drug candidates. Glucuronidation in intestine and liver is an important first-pass drug metabolic pathway, especially for phenolic compounds. This study evaluated the glucuronidation characteristics of several 7-hydroxycoumarin derivatives in beagle dog's intestine and liver in vitro. To this end, glucuronidation rates of 7-hydroxycoumarin (compound **1**), 7-hydroxy-4-trifluoromethylcoumarin (**2**), 6-methoxy-7-hydroxycoumarin (**3**), 7-hydroxy-3-(4-tolyl)coumarin (**4**), 3-(4-fluorophenyl)coumarin (**5**), 7-hydroxy-3-(4-hydroxyphenyl)coumarin (**6**), 7-hydroxy-3-(4-methoxyphenyl)coumarin (**7**), and 7-hydroxy-3-(1H-1,2,4-tirazole)coumarin (**8**) were determined in dog's intestine and liver microsomes, as well as recombinant dog UGT1A enzymes. The glucuronidation rates of **1**, **2** and **3** were 3–10 times higher in liver than in small intestine microsomes, whereas glucuronidation rates of **5**, **6**, **7** and **8** were similar in microsomes from both tissues. In the colon, glucuronidation of **1** and **2** was 3–5 times faster than in small intestine. dUGT1A11 glucuronidated efficiently all the substrates and was more efficient catalyst for **8** than any other dUGT1A. Other active enzymes were dUGT1A2 that glucuronidated efficiently **2**, **3**, **4**, **5**, **6** and **7**, while dUGT1A10 glucuronidated efficiently **1, 2, 3, 4, 5** and **7**. Kinetic analyses revealed that the compounds' K_m values varied between 1.1 (dUGT1A10 and **2**) and 250 μM (dUGT1A7 and **4**). The results further strengthen the concept that dog intestine has high capacity for glucuronidation, and that different dUGT1As mediate glucuronidation with distinct substrates selectivity in dog and human.

1. Introduction

Detailed information about nonclinical and clinical pharmacokinetics (absorption, distribution, metabolism and excretion, ADME) is necessary for all new and existing drugs. Nonclinical ADME data is routinely obtained from rodents, dogs and monkeys [Reichel and Lienau, 2016; Rowland et al., 2015]. Oral bioavailability of drugs and other xenobiotic compounds is critically affected by the extents of absorption and first-pass metabolism in the intestine and liver. Intestinal metabolism is important for bioavailability of compounds that could be directly conjugated, such as glucuronidation of phenols [Gonzalez et al., 2018; Testa et al., 2012].

Glucuronidation is a significant conjugation pathway in the metabolism of drugs, numerous other xenobiotics and endogenous substances such as bilirubin, hormones, bile acids, and retinoids. Glucuronidation is catalyzed by UDP-glucuronosyltransferase enzymes (UGTs, EC 2.4.1.17) and takes place at nucleophilic functional groups on the substrate molecule, particularly hydroxyl, different amino, or carboxylic acid groups. Glucuronide conjugates are subsequently substrates for efflux transporters and are therefore readily excreted in urine or bile [Kaivosaari et al., 2011; Rowland et al., 2013; Wu et al., 2011]. UGTs are membrane bound enzymes of the endoplasmic reticulum and are broadly, but variably expressed in tissues with highest concentrations in the liver and gastrointestinal tract. Per tissue weight, there is a higher concentration of UGTs in the small intestine compared with the liver [Fujiwara et al., 2016; Hu et al., 2014; Naritomi et al., 2015]. On the other hand, at least in humans and at the protein level, only few different UGTs, including extrahepatic ones, are expressed in the small intestine to a level that is detectable by proteomics methods, whereas more UGTs are found in the liver [Sato et al., 2014].

Mammals express four UGT subfamilies. Excluding pseudogenes, nine members of the UGT1A subfamily and ten members of the UGT2A and 2B subfamilies have been identified in human, while ten UGT1As and three UGTs of the 2A and 2B subfamilies have been detected in the dog [http://prime.vetmed.wsu.edu/resources/udp-glucuronsyltransferase-homepage]. The main human UGTs involved in drug metabolism are UGT1A1, UGT1A3, UGT1A4, UGT1A6, UGT1A9, and UGT2B7 [Bock, 2016, Kaivosaari et al., 2011, Rowland et al., 2013], but others, such as UGT1A10, UGT2B10, UGT2B15 and UGT2B17 are also important in different reactions. There are substantial differences in substrate preferences between individual UGTs across species [Komura and Iwaki, 2011; Peters et al., 2016; Troberg et al., 2017]. In the beagle dog three dUGT1A enzymes, 1A2, 1A9 and 1A11, are mainly expressed in intestine and show low or no abundance in the liver, where dUGT2B31 is the most abundantly expressed UGT [Heikkinen et al.,

2015]. Human UGTs 1A7, 1A8, 1A10, 2A1 and 2A2 are all extrahepatic [Court et al., 2012]. Of them, at least UGT1A10 is expressed in the small intestine to high level, along with the (also hepatic) UGTs 1A1, 2B7 and 2B17 [Ohno and Nakajin, 2009; Court et al., 2012; Sato et al., 2014]. Thus, the tissue expression profiles of individual UGTs in human and dog do not match, and it is not possible to correlate exactly between individual human and dog UGTs [Troberg et al., 2015; Heikkinen 2015].

The use of nonclinical species such as beagle dog in predicting human oral bioavailability of drugs has been extensively investigated. In general, bioavailability in animals does not exactly predict quantitatively bioavailability in human. Quantitative (high/low bioavailability) estimates could be improved, when precise species-specific factors that affect human bioavailability are incorporated into the quantitative predictions [Jones et al., 2016; Musther et al., 2014; Peters et al, 2016; Miller et al.; 2019]. In addition, obtaining exact information about pharmacokinetic mechanisms in domestic animals such as beagle dogs is becoming increasingly important in veterinary pharmacotherapy [Anadón, 2016].

We have previously developed a quantitative multiwell plate assay to measure the glucuronidation rate of 7-hydroxy-4-trifluoromethylcoumarin (HFC) [Rahikainen et al., 2013]. Recently we reported six new C3-substituted 7-hydroxycoumarin derivatives that are selective substrates for human UGT1A10 [Juvonen et al., 2018a]. The glucuronidation rate of these substrates was higher in intestine than in liver microsomes. A major advantage of these 7-hydroxycoumarin derivatives as UGT substrates is that their fluorescence properties could be measured in very simple assays, allowing for high-throughput evaluation of enzyme characteristics in different experimental settings.

The aim of this study was to determine glucuronidation characteristics of a panel of C3-substituted 7-hydroxycoumarin derivatives (Figure 1) in dog intestine and liver in vitro and to compare these characteristics to the ones in human.

2. Materials and methods

2.1. Reagents: Alamethicin, UDP-glucuronic acid sodium salt, 7-hydroxycoumarin (compound **1**) (99%), HFC (**2**) (99%), 6-methoxy, 7-hydroxycoumarin (**3**) (99 %) were from Sigma-Aldrich (Mannheim, Germany). $MgCl_2$ were from Riedel-de Haen (Vantaa, Finland). Water was deionized by MilliQ gradient A10.

The novel 7-hydroxycoumarin derivatives 3-triazole-7-hydroxycoumarin (**8**), 3-(4-tolyl)-7-hydroxycoumarin (**4**), 3-(4-fluorophenyl-7-hydroxycoumarin (**5**), 3-(4-methoxyphenyl)-7-hydroxycoumarin (**7**), 3-(4-hydroxyphenyl)-7-hydroxycoumarin (**6**) were synthesized using the Perkin-Oglialor condensation reaction described in detail earlier [Juvonen et al., 2018b].

2.2. Biological materials: Beagle dog necropsy was performed at F. Hoffmann-La Roche Ltd (Nutley, NJ) according to institutional guidelines and in compliance with national and regional legislation. For detailed description of the preparation of intestine and liver microsomal samples of beagle dogs see [Heikkinen et al., 2015]. Liver samples were snap frozen in liquid nitrogen and stored at $-80°C$ before sample preparation. Small intestines were divided into five equal segments (median length 53 cm), and colon (median length 29 cm) were collected as separate anatomical segments.

Ten recombinant dog UGT1As, namely 1A1, 1A2, 1A3, 1A4, 1A6, 1A7, 1A8, 1A9, 1A10 and 1A11, were produced as His-tagged proteins in baculovirus-infected insect cells and expression normalized as previously described [Troberg et al., 2015]. The relative expression levels of each of these recombinant UGTs were the following: 1 for dUGT1A1, 6.5 for dUGT1A2, 3.7 for dUGT1A3, 5.8 for dUGT1A4, 14.6 for dUGT1A6, 17.9 for dUGT1A7, 1.3 for dUGT1A8, 7.3 for dUGT1A9, 3.8 for dUGT1A10 and 10.1 for dUGT1A11.

2.3. Glucuronidation assays: The assays were carried out in 96 multiwell plates, and incubations were done in 100 µl and at 37°C, in the presence of 100 mM Tris-HCl buffer pH 7.4, 0.5 mM UDPGA, 0.1 – 0.4 g/l protein intestine or liver microsomes or 0.04 - 1 g/l protein recombinant UGT and the tested 7-hydroxycoumarin derivative at the indicated concentrations. Alamethicin (25 µg/ml) was present at microsomal incubation but not at incubations of recombinant UGTs. Blank samples did not contain either UDPGA or enzyme source. Fluorescence decline in the multiwell plate experiments was monitored every other minute, for 40 min, using an excitation at 405 nm and detecting emission at 460 nm, in a Victor[2] 1420 Multilabel counter (PerkinElmer, Life Sciences, Turku, Finland) [Juvonen et al. 2018a].

The fluorescence values were transformed into molarity using standard curves that were prepared with the respective compounds at every time point (fluorescence disappeared upon glucuronidation). Slopes of the substrate concentration decrease per min were calculated using linear regression analysis, in which the linear part of the kinetic assay indicated the glucuronidation rate. Enzyme catalyzed glucuronidation rate was calculated by subtracting the blank value from the

full reaction value and then normalized by diving the amount of protein in the sample. The intra-assay variability of the kinetic assays was 6 % when compound **8** was used as the substrate.

Kinetic analyses were also performed in the same 96 multiwell plate assays, with excitation at 405 nm and detection at 460 nm, using eleven concentrations per substrate (0.25–20 μM). The reactions were catalyzed linearly for at least 15 min even at the lowest substrate concentrations. The data was analyzed by the Michaelis-Menten equation $v = S * V_{max} /(K_m + S)$, in which v is the reaction rate at substrate concentration (S), V_{max} is limiting rate of the reaction and K_m is the Michaelis constant equal to the substrate concentration, at which the reaction rate is 50 % of V_{max} .

For multivariate analysis, we did principal component analysis (PCA) using SIMCA 15.0.2 (Umetrics). For analysis of 7-hydroxycoumarin derivatives glucuronidation in dog intestine and liver microsomes, we first normalized the values within samples from the same UGT or dog glucuronidating the same substrate, so that all values were divided by the highest value (normalized value = value / max value), due to large variation in glucuronidation rate between samples from different UGTs or dogs.

3. Results

At first, we screened the glucuronidation rates of 7-hydroxycoumarin (**1**) and its seven derivatives by the dog recombinant dUGT1As, i.e. 1A1, 1A2, 1A3, 1A4, 1A6, 1A7, 1A8, 1A9, 1A10 and 1A11 using a substrate concentration of 10 μM in each case (Figure 2, Table 1). The results revealed the highest rate for compound **5** by dUGT1A2 (169 nmol/(min*g protein)), which glucuronidated also **2** almost equally fast. Compounds **8** and **1** were glucuronidated at the lowest rates by the dUGT1A enzymes. The number of dUGT1As catalyzing glucuronidation of individual compounds varied. For example, **8** was glucuronidated preferentially by dUGT1A11 with some contribution by dUGT1A1 and minor contribution by the other enzymes. The other derivatives were glucuronidated by three or more dUGT1As.

dUGT1A11 glucuronidated all eight compounds, while the other dUGT1As exhibited more restricted substrate profiles, at least in the case of this group of compounds (Figure 2, Table 1). dUGT1A2 and dUGT1A10 glucuronidated six different compounds. dUGT1A4 and dUGT1A9 did not catalyze any, or catalyzed only poorly few of the compounds. The data was analyzed by the PCA model, which used five components with a cumulative R^2X of 0.95, and a cumulative Q^2 of 0.58. dUGTs 1A1, 1A3, 1A4, 1A6, 1A7, 1A8 and 1A9 formed a separate group in the analysis,

having a weak connection with all substrates (Figure 3). dUGT1A2 had a strong connection with substrates **4**, **5**, **6** and **7**, whereas dUGT1A10 and dUGT1A11 had a strong connection with substrates **1**, **3** and **8**. Substrate **2** had an equal connection with dUGT1A2, dUGT1A10 and dUGT1A11.

Michaelis-Menten kinetic parameters were determined for the fastest glucuronidation reactions (Table 2, Supplement Figure 1). The derived K_m values varied between 1.1 μM (compound **2** - dUGT1A10) and 250 μM (**4** - dUGT1A7). In most cases the K_m values were lower for dUGT1A10 and dUGT1A11 than in the other dUGTs which catalyzed the same reactions. Most K_m values were below 10 μM, particularly for dUGT1A10 and dUGT1A11. Higher K_m values were observed for **1** (dUGT1A6, dUGT1A11), **2** (dUGT1A2), **3** (dUGT1A1, dUGT1A2), and **4** (dUGT1A3, dUGT1A7). Normalized intrinsic clearance (V_{max}/K_m ratio) varied 100-fold (1.8–180 ml/(min*g protein)). Normalized intrinsic clearance was highest for glucuronidation of **5** by dUGT1A1 and lowest for **3** by dUGT1A1 (Table 3).

Alongside the study on recombinant dUGT1As, glucuronidation rates of the same eight compounds were measured in dog intestine and liver microsomes. A comparison between the rates in these tissues shows that compounds **1**, **2** and **3** were glucuronidated 3–10 times faster in liver microsomes than in microsomes of segment 2 of the small intestine (Figure 4A). The glucuronidation rates of **5**, **6**, **7** and **8** were almost equal between liver and intestine segment 2 microsomes.

To evaluate glucuronidation in different segments of the intestine, the enzyme activity was measured for compounds **1**, **2**, **5** and **8** in microsomes from five equally long segments of the small intestine (S1–S5) and colon (S6), from four dogs. Glucuronidation rate of **8** was higher in segments 1–5 than in colon and liver (Figure 4B). The glucuronidation rate of **5** was almost equal in segments 3–4 and colon, while it was somewhat lower in segments 1–2, 5 and liver (Figure 4C). For **1** and **2** the rates were higher in colon and liver than in segments 1–5 (Figure 4D, 4E). The data was analyzed by the PCA model with five components (cumulative $R^2X = 0.99$ and cumulative $Q^2 = 0.77$). Compounds **1** and **2** were strongly connected with liver and colon microsomes, while compound **8** with intestine microsomes, whereas the connection of compound **5** was stronger with intestine than with liver microsomes (Figure 5).

The effect of concentrations of compounds **1**, **2** and **5** on glucuronidation rate was evaluated in the dog intestine and liver microsomes. The shapes of the curves were compatible with the Michaelis-Menten equation. The goodness of fit was high for both intestine and liver glucuronidation of all three compounds (Table 4, Supplement Figure 2). Eadie-Hofstee analyses revealed deviation from a

single enzyme glucuronidation kinetics, particularly in the liver microsomal samples (Supplement Figure 2). The K_m values of all compounds were lower for intestine than liver microsomes. The V_{max} value and intrinsic clearance of compound **5** glucuronidation were higher in the intestine than liver microsomes. On the other hand, V_{max} and intrinsic clearance of compounds **1** and **2** were higher in liver than intestine microsomes.

4. Discussion

Phenolic compounds undergo efficient first-pass elimination by glucuronidation in the intestine and liver of both humans and animals [Mizuma, 2009; Ritter, 2007; Wu et al., 2011]. In this study we have evaluated the glucuronidation characteristics of phenolic 7-hydroxycoumarin and seven of its derivatives. The glucuronidation of these eight phenolic compounds was examined in intestine and liver microsomes of beagle dogs, and in ten individual dog UGT1A enzymes. The study yielded many interesting results, such as 1) the glucuronidation rates of several derivatives, e.g. **5**, **6**, **7** and **8,** were almost equal in intestine and liver microsomes, while the rates of compounds **1**, **2** and **3** were clearly faster in liver than in intestine microsomes, 2) compound **8** was a largely selective substrate for dUGT1A11, 3) the glucuronidation of most derivatives was catalyzed by several different dUGT1As at different rates, but dUGT1A2, dUGT1A10 and dUGT1A11 exhibited higher efficiency in most cases. Taken together, these results demonstrate that phenolic substrates could be glucuronidated efficiently in tissues responsible for first pass metabolism in dog, namely intestine and liver. In addition, preliminary information was obtained about the relationships between the structure of 7-hydroxycoumarin derivatives and glucuronidation capacity by individual dUGT1As.

The nomenclature of human UGT1As developed following some differences of opinions and co-discoveries, resulting in a situation where the UGTs on the large *ugt1a* gene are numbered according to their order (their exon ones actually) only until UGT1A7 [MacKenzie et al., 2005]. Then comes UGT1A10 and only after it UGT1A8, with pseudogenes being present both between UGT1A9 and UGT1A10 and downstream of UGT1A8. In rat, mouse and dog the UGT1A genes are named according to the order of their first exons on the large gene [MacKenzie et al., 2005; Troberg et al., 2015]. This means that the differences between dog and human UGT1As start from the names/order of UGTs 1A8 and higher numbers. In addition, the human UGTs 1A2 and 1A11 (as well as h1A12 and h1A13) are pseudogenes, whereas in dog they are expressed. It has become evident in earlier studies that similarly named UGTs in dog and human do not glucuronidate various substrates in the same way [Heikkinen et al., 2015; Komura and Iwaki, 2011; Troberg et al. 2015],

e.g. entacapone is glucuronidated efficiently by the hepatic hUGT1A9, while in dog it is mainly conjugated by the intestinal dUGT1A11 [Troberg et al., 2015]. It thus seems that the enzyme's name is not the only reason for differences in activity, it must be also tissue of expression and some variability in protein sequence, even if they are largely homologous.

The present study further confirmed this difficulty when comparing human and dog UGTs (Table 5). For example, compound **8**, a selective substrate for human UGT1A10 [Juvonen et al., 2018a], was not glucuronidated by dUGT1A10, but showed affinity and partial selectivity for dUGT1A11. Compounds **5**, **6**, and **7** are glucuronidated predominantly by hUGT1A10 in human, whereas in dog all of them were catalyzed by several dUGT1As. Thus, glucuronidation of these 7-hydroxycoumarin derivatives in human is more restricted to fewer UGT1As than in dog.

Glucuronidation of **5, 6, 7** and **8** was fast both in dog and human small intestine (Table 5). In dog the reaction was catalyzed efficiently by extrahepatic dUGT1A11, which is abundantly expressed in the intestine [Heikkinen et al., 2015]. Compounds **5**, **6**, and **7** were also glucuronidated by dUGT1A2, which is also abundantly expressed in the small intestine, but also expressed in the liver at low level. Expression of dUGT1A2 and dUGT1A11 in the intestine explain the high glucuronidation rates of **5**, **6**, and **7**. In human these 7-hydroxycoumarins are glucuronidated several times faster in the intestine than in liver due to abundant expression of UGT1A10 in intestine and its selectivity for these compounds [Juvonen et al., 2018a]. These results demonstrate that **5**, **6**, **7** and **8** are only partially selective substrates for small intestinal glucuronidation in dog. Glucuronidation of compounds **1, 2, 5** and **8** occurred in the colon at rates comparable to liver.

Compounds **1, 2** and **3** were glucuronidated faster and with a higher intrinsic clearance in dog liver than intestine microsomes, catalyzed particularly by dUGT1A10 and d1A11, but also by some other dUGTs such as dUGT1A2 and d1A6. Compounds **1** and **2** are also glucuronidated faster in human liver than intestine. Both **1** and **2** are glucuronidated efficiently by human UGT1A6 [Juvonen et al., 2018a]. Compound **3** (6-methoxy-7-hydroxycoumarin, scopoletin) is glucuronidated by several human UGTs, the most efficient being hUGT1A10 [Juvonen et al., 2019]. A comparison of glucuronidation rate of **3** between human liver and intestine microsomes has not been done. Alongside dUGT1As, dUGT2B31 is known to be expressed in dog liver and its expression level is higher than dUGT1As. It is currently not known whether UGT2B31 contributes to the glucuronidation of 7-hydroxycoumarin derivatives used in this study. Currently, it remains unresolved what dUGT(s) is exactly responsible for the higher glucuronidation rate of **1, 2** and **3** in dog's liver than in its intestine microsomes.

The substrate specificity and particularly the kinetic analyses with recombinant dUGT1As may also teach us about properties of the substrate binding site of these enzymes. The K_m values of the compounds is dependent on their binding modes to the active sites in individual UGTs. The relationships between compound's structure and UGT active sites determine the glucuronidation selectivity and rate [Juvonen et al., 2018a]. dUGT1A11 glucuronidated all eight tested compounds. The K_m of compound **1** for dUGT1A11 glucuronidation was 5–13 times higher than for the other seven compounds, indicating that substituents at positions 3, 4 or 6 of the 7-hydroxycoumarin scaffold increased the binding affinity. In contrast, these substituents abolished glucuronidation of compound **1** by dUGT1A6. A 3-triazole substituent of 7-hydroxycoumarin shifted the compound selectivity for dUGT1A11. The 7-hydroxycoumarin structure with several different kinds of phenyl substituents at position 3 were glucuronidated well by dUGT1A2, dUGT1A10 and dUGT1A11. However, a 4-hydroxyphenyl substituent abolished glucuronidation by dUGT1A10, dUGT1A4 and dUGT1A9 did not glucuronidate 7-hydroxycoumarin or its derivatives that were substituted at positions 3, 4 or 6. This brief analysis suggests that the active sites of dUGT1A11, dUGT1A10 and dUGT1A2 are more flexible than the other dUGT1As, as they accepted many kinds of 7-hydroxycoumarin derivatives.

5. Conclusions

Simple and quantitative assays for glucuronidation rate of fluorescent 7-hydroxycoumarin derivatives were applied to ten recombinant dog UGT1As, as well as canine intestine and liver microsomes. Compounds **4**, **5**, **6**, **7** and **8** were glucuronidated equally fast in small intestine and liver microsomes. Glucuronidation of these compounds was catalyzed efficiently by intestinal UGT1A2 and UGT1A11. Compounds **1**, **2** and **3** were glucuronidated faster in liver than small intestine, and among the recombinant enzymes they were glucuronidated most efficiently by dUGT1A10, followed by dUGT1A2 and dUGT1A11. The results highlight the high capacity of dog intestine and colon for glucuronidation, and reveals that different UGTs mediate glucuronidation with distinct substrates selectivity in dog and human, even if all the substrates are 7-hydroxycoumarin derivatives. Because compound 8 was efficiently and selectively glucuronidated by dUGT1A11, it can be used as the probe substrate for dUGT1A11 to study its expression in other dog tissues or to screen potential inhibitors of the enzyme.

Declaration of competing interest

All authors declare no conflict of interest

Credit author statement

Risto O. Juvonen: Conceptualization, validation, formal analysis, investigation, writing-original draft, writing-review & editing, visualization, project administration. **Aki T. Heikkinen**: resources, writing-review & editing. **Olli Kärkkäinen**: data curation, writing-review & editing, visualization. **Rabia Jehangir**: investigation, writing-review & editing, **Juhani Huuskonen**: resources, writing-review & editing, **Johanna Troberg**: methodology, resources, writing-review & editing, **Hannu Raunio**: writing-original draft, writing-review & editing, funding administration. **Olli T. Pentikäinen**: resources, writing-review & editing, **Moshe Finel:** methodology, resources, writing-review & editing, funding administration.

References

Anadón A. Perspectives in Veterinary Pharmacology and Toxicology. Front Vet Sci. 2016;3:82.

Bock KW. The UDP-glycosyltransferase (UGT) superfamily expressed in humans, insects and plants: Animal-plant arms-race and co-evolution. Biochem Pharmacol. 2016;99:11-7.

Court MH, Zhang X, Ding X, Yee KK, Hesse LM, Finel M. Quantitative distribution of mRNAs encoding the 19 human UDP-glucuronosyltransferase enzymes in 26 adult and 3 fetal tissues. Xenobiotica. 2012;42(3):266-77.

Gonzalez FJ, Coughtrie M, Tukey RH. Drug metabolism. In: Goodman & Gilmans's The Pharmacological Basis of Therapeutics. Brunton LL. Hilal-Dandan R, Knollman BC, Editors. 13th Edition, pp. 85-100. McGraw-Hill, New York 2018.

Fujiwara R, Yokoi T, Nakajima M. Structure and Protein-Protein Interactions of Human UDP-Glucuronosyltransferases. Front Pharmacol. 2016;7:388. eCollection 2016.

Heikkinen AT, Friedlein A, Matondo M, Hatley OJ, Petsalo A, Juvonen R, Galetin A, Rostami-Hodjegan A, Aebersold R, Lamerz J, Dunkley T, Cutler P, Parrott N. Quantitative ADME proteomics - CYP and UGT enzymes in the Beagle dog liver and intestine. Pharm Res. 2015;32(1):74-90.

Hu DG, Meech R, McKinnon RA, Mackenzie PI. Transcriptional regulation of human UDP-glucuronosyltransferase genes. Drug Metab Rev. 2014;46(4):421-58.

Jones CR, Hatley OJ, Ungell AL, Hilgendorf C, Peters SA, Rostami-Hodjegan A. Gut Wall Metabolism. Application of Pre-Clinical Models for the Prediction of Human Drug Absorption and First-Pass Elimination. AAPS J. 2016;18(3):589-604.

Juvonen RO, Rauhamäki S, Kortet S, Niinivehmas S, Troberg J, Petsalo A, Huuskonen J, Raunio H, Finel M, Pentikäinen OT. Molecular Docking-Based Design and Development of a Highly Selective Probe Substrate for UDP-glucuronosyltransferase 1A10. Mol Pharm. 2018a;15(3):923-933.

Juvonen RO, Ahinko M, Huuskonen J, Raunio H, Pentikäinen OT. Development of New Coumarin-Based Profluorescent Substrates for Human Cytochrome P450 Enzymes. Xenobiotica. 2018b Oct 1:1-27. doi: 10.1080/00498254.2018.1530399. [Epub ahead of print]

Juvonen RO, Novák F, Emmanouilidou E, Auriola S, Timonen J, Heikkinen AT, Küblbeck J, Finel M, Raunio H. Metabolism of Scoparone in Experimental Animals and Humans. Planta Med. 2019;85(6):453-464.

Kaivosaari S, Finel M, Koskinen M. N-glucuronidation of drugs and other xenobiotics by human and animal UDP-glucuronosyltransferases. Xenobiotica. 2011;41(8):652-69.

Komura H, Iwaki M. In vitro and in vivo small intestinal metabolism of CYP3A and UGT substrates in preclinical animals species and humans: species differences. Drug Metab Rev. 2011;43(4):476-98.

Mackenzie PI, Bock KW, Burchell B, Guillemette C, Ikushiro S, Iyanagi T, Miners JO, Owens IS, Nebert DW. Nomenclature update for the mammalian UDP glycosyltransferase (UGT) gene superfamily. Pharmacogenet Genomics. 2005;15(10):677-85.

Miller, N.A., Reddy, M.B., Heikkinen, A.T., Lukacova, V., Parrott, N. Physiologically Based Pharmacokinetic Modelling for First-In-Human Predictions: An Updated Model Building Strategy

Illustrated with Challenging Industry Case Studies. Clinical Pharmacokinetics. 2019. 58(6): 727-746.

Mizuma, T., Intestinal glucuronidation metabolism may have a greater impact on oral bioavailability than hepatic glucuronidation metabolism in humans: A study with raloxifene, substrate for UGT1A1, 1A8, 1A9, and 1A10. *Int J Pharmaceut* **2009,** *378* (1-2), 140-141.

Musther H, Olivares-Morales A, Hatley OJ, Liu B, Rostami Hodjegan A. Animal versus human oral drug bioavailability: do they correlate? Eur J Pharm Sci. 2014;57:280-91.

Naritomi Y, Nakamori F, Furukawa T, Tabata K. Prediction of hepatic and intestinal glucuronidation using in vitro-in vivo extrapolation. Drug Metab Pharmacokinet. 2015;30(1):21-9.

Ohno S, Nakajin S. Determination of mRNA expression of human UDP-glucuronosyltransferases and application for localization in various human tissues by real-time reverse transcriptasepolymerase chain reaction. Drug Metabolims and Disposition 2009;37(1), 32-44.

Peters SA, Jones CR, Ungell AL, Hatley OJ. Predicting Drug Extraction in the Human Gut Wall: Assessing Contributions from Drug Metabolizing Enzymes and Transporter Proteins using Preclinical Models. Clin Pharmacokinet. 2016;55(6):673-96.

Rahikainen T, Häkkinen MR, Finel M, Pasanen M, Juvonen RO. A high throughput assay for the glucuronidation of 7-hydroxy-4-trifluoromethylcoumarin by recombinant human UDP-glucuronosyltransferases and liver microsomes. Xenobiotica. 2013;43(10):853-61.

Reichel A, Lienau P. Pharmacokinetics in Drug Discovery: An Exposure-Centred Approach to Optimising and Predicting Drug Efficacy and Safety. Handb Exp Pharmacol. 2016;232:235-60.

Ritter, J. K. Intestinal UGTs as potential modifiers of pharmacokinetics and biological responses to drugs and xenobiotics. Expert Opin. Drug Metab. Toxicol. 2007, 3 (1), 93−107.

Rowland A, Miners JO, Mackenzie PI. The UDP-glucuronosyltransferases: their role in drug metabolism and detoxification. Int J Biochem Cell Biol. 2013;45(6):1121-32.

Rowland M, Lesko LJ, Rostami-Hodjegan A. Physiologically Based Pharmacokinetics Is Impacting Drug Development and Regulatory Decision Making. CPT Pharmacometrics Syst Pharmacol. 2015;4(6):313-5.

Sato, Y.; Nagata, M.; Tetsuka, K.; Tamura, K.; Miyashita, A.;Kawamura, A.; Usui, T. Optimized Methods for Targeted Peptide-Based Quantification of Human Uridine 5 ′-Diphosphate-Glucuronosyltransferases in Biological Specimens Using Liquid Chromatography-Tandem Mass Spectrometry. Drug Metab. Dispos. 2014, 42 (5),885−889.

Testa B, Pedretti A, Vistoli G. Reactions and enzymes in the metabolism of drugs and other xenobiotics. Drug Discov Today. 2012;17(11-12):549-60.

Troberg J, Jävinen, Ge B-G, Young L. Finel M. UGT1A10 Is a High Activity and Important Extrahepatic Enzyme: Why Has Its Role in Intestinal Glucuronidation Been Frequently Underestimated? Molecular Pharmaceutics. 2017, 14(9): 2875-2883.

Troberg J, Järvinen E, Muniz M, Sneitz N, Mosorin J, Hagström M, Finel M. Dog UDP-glucuronosyltransferase enzymes of subfamily 1A: cloning, expression, and activity. Drug Metab Dispos. 2015;43(1):107-18.

Wu B, Kulkarni K, Basu S, Zhang S, Hu M. First-pass metabolism via UDP-glucuronosyltransferase: a barrier to oral bioavailability of phenolics. J Pharm Sci. 2011;100(9):3655-81.
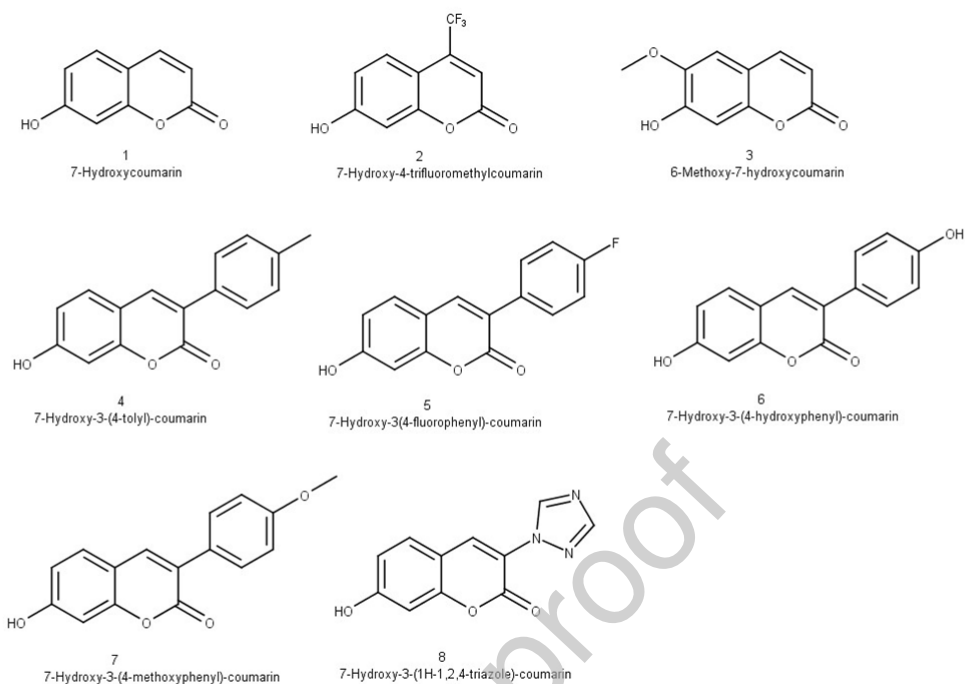
Figure legends

Figure 1.

Figure 1. Structures of the 7-hydroxycoumarin derivatives.
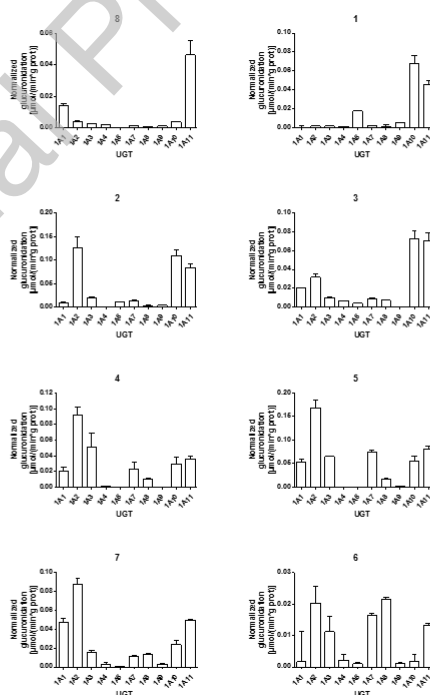
Figure 2.

Figure 2. Glucuronidation of eight 7-hydroxycoumarin derivatives by ten dog UGT1A enzymes. Glucuronidation was determined at 10 µM substrate concentration.

Figure 3: Biplot of the principal component analysis (PCA) of eight 7-hydroxycoumarin derivative glucuronidation by dog UGT1As. The biplot shows scores for enzyme activity means and loadings for the two first latent components of the PCA model explaining 39% and 26% of the variance in the data, respectively. Substrates are shown as blue circles and UGT1A enzymes as black hexagons.

Figure 4.

Figure 4. Glucuronidation of 7-hydroxycoumarin derivatives in microsomes of dog small intestine (S1–S5), colon (S6) and l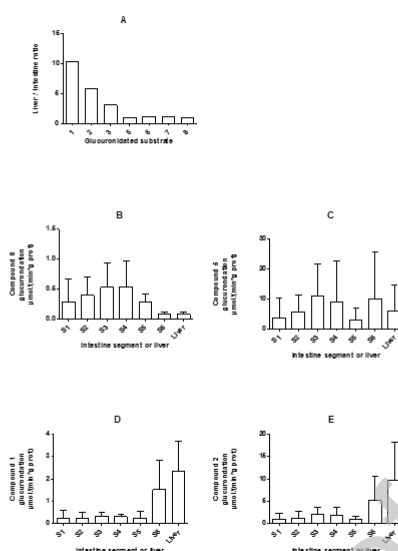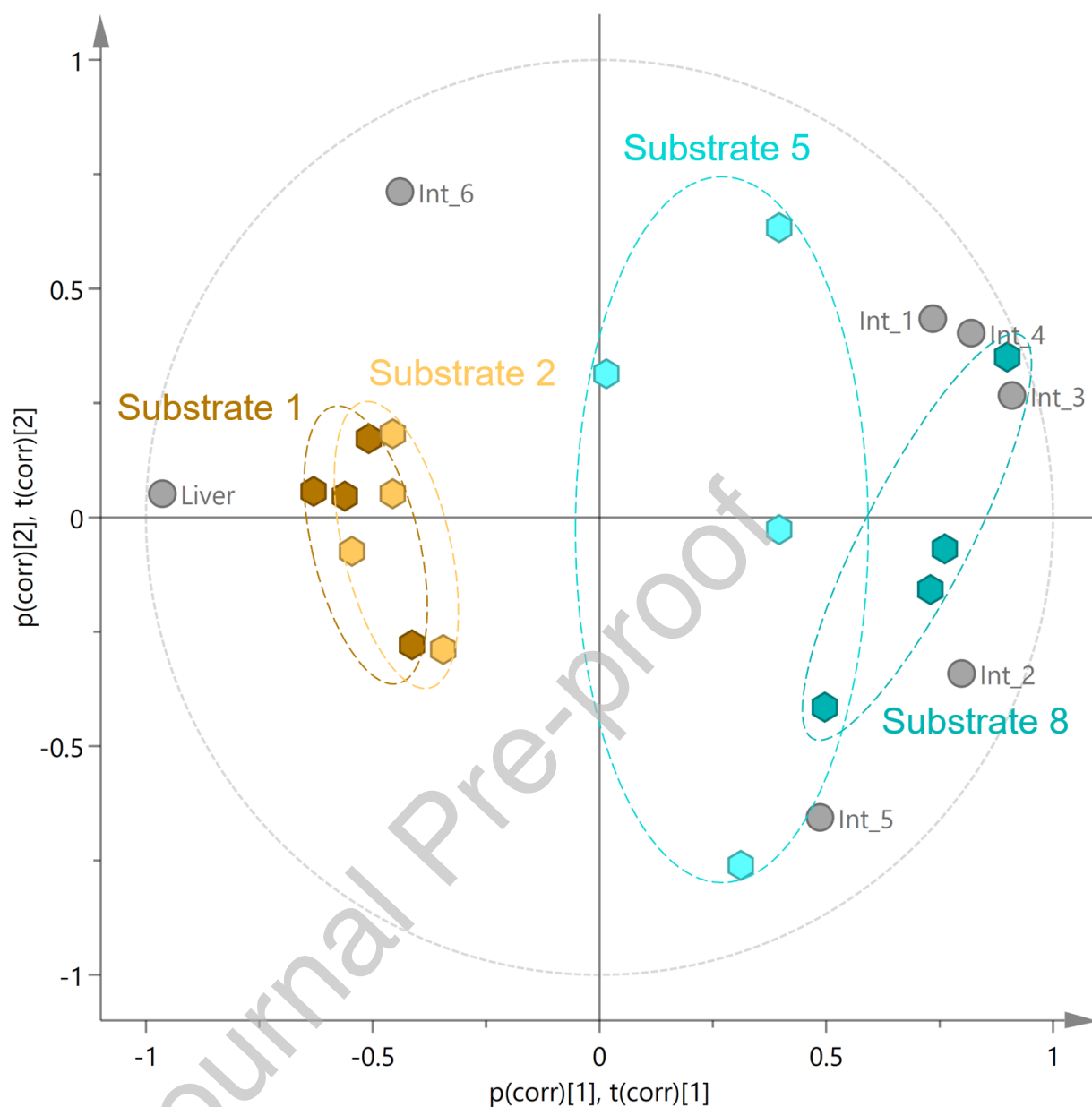iver. Panel A shows the ratio of glucuronidation rates between liver and intestine segment 2 at 10 µM substrate concentration in one dog. Panels B – C show the glucuronidation rate of the indicated substrates in microsomes of intestinal segment or liver (means of four different dogs).

Figure 5. Biplot of the principal component analysis model of glucuronidation of 7-hydroxycoumarin derivatives in microsomes of dog intestine or liver. First two components (explaining 58% and 21% of variance, respectively) of a PCA model (5 components, cumulative $R^2X = 0.99$, cumulative $Q^2 = 0.77$). Substrates **1** (brown hexagons) and **2** (orange hexagons) show association with liver microsomes and substrates **5** (light blue hexagons) and **8** (dark blue hexagons) with intestine microsomes (sample types shown as gray circles).

Supplement figure 1. Michaelis-Menten plots of glucuronidation of eight 7-hydroxycoumarin derivatives by the most efficient dog UGT enzymes.

Supplement figure 2. Michaelis-Menten plots and Eadie-Hofstee analysis of glucuronidation of compounds 1, 2 and 5 by the liver and intestine segment 2 microsomes.

Table 1. Glucuronidation of eight 7-hydroxycoumarin derivatives by ten dog UGT enzymes. Glucuronidation rate (nmol/(min*g protein) was determined at 10 µM substrate concentration. The substrates are organized according to the selectivity with compound **8** showing most selectivity (for UGT1A11). Substrates on the right are the least selective. The grey scale indicates the rate of glucuronidation (white = lowest; black = highest).

UGT	Substrate							
	8	1	3	2	7	4	5	6
1A1	14	0	20	9	48	21	53	2
1A2	4	1	32	125	88	92	169	20
1A3	2	2	10	20	16	51	65	11
1A4	2	1	7	0	3	1	-2	2
1A6	0	17	4	11	0	0	-1	1
1A7	1	2	9	13	11	23	74	16
1A8	0	1	7	4	14	10	17	21
1A9	1	5	-6	4	3	-1	3	1
1A10	4	68	73	110	24	30	56	2
1A11	46	45	70	84	50	36	82	13

Table 2. Michaelis-Menten kinetic constants of glucuronidation of different 7-hydroxycoumarin substrates by dog UGT1A enzymes.

dUGT1A	Compound	K_m (95 % confidence limits) µM	V_{max} (95 % confidence limit) Normalized rate µmol/(min*g protein)
1	8	3.6 (2.0-5.2)	0.012 (0.009-0.014)
11	8	1.8 (1.2-2.5)	0.049 (0.043-0.055)
2	2	10.2 (6.5-14)	0.19 (0.15-0.22)
10	2	1.1 (0.5-1.7)	0.10 (0.09-0.11)
11	2	3.1 (1.7-4.6)	0.078 (0.07-0.09)
6	1	22 (11-33)	0.18 (0.12-0.24)
10	1	5.1 (3.2-7.1)	0.24 (0.21-0.28)
11	1	17 (11-23)	0.31 (0.25-0.38)
2	6	4.3 (3.6-5.1)	0.074 (0.67-0.08)
7	6	4.9 (2.8-7.0)	0.035 (0.029-0.040)
11	6	2.5 (0.99-4.1)	0.056 (0.043-0.068)
1	7	5.5 (4.1-6.9)	0.072 (0.065-0.080)
2	7	9.9 (6.4-13)	0.24 (0.2-0.28)
10	7	4.3 (2.1-6.5)	0.056 (0.046-0.067)
11	7	2.1 (1.6-2.8)	0.072 (0.066-0.078)
1	3	40 (0-167)	0.071 (0-0.24)
2	3	87 (0-320)	0.29 (0-0.92)
10	3	2.4 (1.7-3.0)	0.096 (0.089-0.10)
11	3	4.6 (3.6-5.7)	0.16 (0.15-0.18)
2	4	7.2 (4.3-10)	0.21 (0.17-0.25)
3	4	19 (4-35)	0.24 (0.12-0.36)
7	4	250 (0-1270)	1.6 (0-7.6)
10	4	5.0 (2.1-7.9)	0.081 (0.063-0.099)
11	4	1.7 (0.86-2.6)	0.086 (0.075-0.098)
1	5	2.6 (1.4-3.9)	0.48 (0.41-0.56)
2	5	4.2 (3.5-4.9)	0.20 (0.18-0.21)
3	5	9.4 (6.2-11)	0.18 (0.15-0.21)
7	5	8.5 (7.0-10)	0.051 (0.047-0.055)
10	5	3.8 (2.4-5.2)	0.093 (0.082-0.1)
11	5	1.3 (1.4-2.1)	0.10 (0.094-0.11)

Table 3. Comparison of normalized intrinsic clearances. The values (V_{max}/K_m) were calculated from the data in Table 2.

dUGT	Normalized intrinsic clearance of compounds ml/(min*g protein)							
	8	1	2	6	3	7	4	5
1A1	3.3	ND	ND	ND	1.8	13	ND	180
1A2	ND	ND	19	17	3.3	24	29	48
1A3	ND	ND	ND	ND	ND	ND	13	19
1A4	ND	ND	ND	ND	ND	ND	ND	ND
1A6	ND	8.2	ND	ND	ND	ND	ND	ND
1A7	ND	ND	ND	7.1	ND	ND	6.4	6
1A8	ND	ND	ND	ND	ND	ND	ND	ND
1A9	ND	ND	ND	ND	ND	ND	ND	ND
1A10	ND	47	91	ND	40	13	16	24
1A11	27	18	25	22	35	34	51	77

ND = Not determined, because glucuronidation rate was low at 10 µM compound screening.

Table 4. Michaelis-Menten kinetic constants of glucuronidation of substrates **1, 2** and **5** by intestine and liver microsomes of dogs.

Microsomes	Compound	K_m (95 % confidence limit) μM	V_{max} (95 % confidence limit) μmol/(min*g protein)	Vmax / Km L/(min*g protein)	R square
Intestine	**5**	4.3 (1.6–7.0)	3.3 (2.6–4.1)	0.77	0.9334–0.9877
Liver	**5**	12.8 (7.5–18.1)	2.4 (1.9–3.0)	0.19	0.9440–0.9953
Intestine	**1**	40 (0–129)	0.93 (0–2.5)	0.023	0.9789–0.9982
Liver	**1**	77 (0–162)	10.5 (0.8–20.1)	0.14	0.9859–0.9963
Intestine	**2**	14 (0–32)	2.2 (0.6–3.7)	0.15	0.9916–0.9964
Liver	**2**	120 (0–270)	44 (0–93)	0.36	0.9975–0.9995

Table 5. Comparison of glucuronidation of 7-hydroxycoumarin derivatives between dog and human. The human data is from the studies Juvonen et al. 2018a and Juvonen et al. 2019.

	Liver/intestine ratio	Liver/Intestine ratio	The most efficient dUGT	The most efficient hUGT
7-Hydroxy-coumarin derivative	**Dog**	**Human**	**Dog**	**Human**
1	>3	>3	1A10, 1A11>1A6	1A6>1A9, 1A10
2	>3	>2	1A2, 1A10, 1A11	1A6, 1A10>1A7, 1A9, 2A1
3	>3	ND	1A10, 1A11 > 1A1, 1A2	1A6>1A7, 1A8, 1A9, 1A10, 2B17
4	ND	ND	1A2> 1A3> 1A1, 1A7, 1A10, 1A11	1A10
5	≈1	<1	1A2> 1A1, 1A3, 1A7, 1A10, 1A11	1A10>>1A1
6	≈1	<1	1A2, 1A7, 1A8>1A3, 1A11	1A10>>1A1
7	ND	<1	1A2> 1A1, 1A11 > 1A3, 1A7, 1A8, 1A10	1A10>>1A1
8	≈1	<1	1A11>1A1	1A10

ND means not determined.

GRAPHICAL_ABSTRACT